

Determination of the Specifically Surface of Thin Films by Héron of Alexandria Relationship

^{1,2}Y. Thimont and ¹K. Croué

¹Laboratoire de Réactivité et de Chimie des Solides
UMR CNRS 6007, 33, rue Saint-Leu
80039 Amiens, France

²Laboratoire de Cristallographie et de Sciences des Matériaux
UMR CNRS 6508, 6, Boulevard du Maréchal Juin 14050 Caen, France

Abstract

The determination of the specifically surface of thin films is crucial in many cases, but it can be problematic for complex surface (no geometric shapes). This work presents a method employed for the calculation of the specifically surface of thin films using atomic force microscope data. After the presentation of the mathematical model and how the program performs, we use simple geometric surfaces to discuss the coherence and the efficiency of our method. In the second part, we have experimentally measured the specifically surface of two samples. The specifically surface of the first sample (consisting in easily geometric shapes) has been calculated by our program and results have been confirmed by another mathematical approximation calculation. For the second sample its important roughness was not suitable with the approximation whereas coherent results were only obtained with our method.

Keywords: Specifically surface, Atomic Force Microscopy, FORTRANTM

1. Introduction

The determination of the specifically surface of thin films is a crucial aim for many applications such as gas sensors. In this domain, the main experimental technique employed in this domain is that a Brunauer Emmett and Teller (BET), the picnometry, but these techniques need an important quantity of matter and aren't always accurate. Other techniques like TEM analysis have been developed but always in the case of powder samples. Thus in summary, very few techniques are

devoted to the determination of the specifically surface of thin films [6]. AFM is a commonly used method employed for morphology characterisation of thin film surfaces and the determination of the growth mechanism's. This work proposes a new method for thin film specifically surface determination using atomic force microscope (AFM) data [1][8]. Often the AFM apparatus is used to determine morphology of thin films surface [2][4]. Surfaces are characterized by a topographic picture and statistical data such as the roughness of the surface by rms calculation, the amplitude distribution, the Fast Fourier Transformation (FFT), the maximum peak to valley. Nevertheless, no AFM data's are devoted to the specifically surface. Herein, we present a mathematical approach which includes the matrix calculation of the AFM data and developed a new software for the specifically surface of thin film calculation.

2. Theoretical approach

2.1. The mathematical development

The determination of surfaces can be easily calculated with the derivative calculation of three dimensions functions, but in specifically cases, like with AFM data, no functions can be extracted. An AFM measurement is a determination of a z amplitude fixed for one (x,y) coordinate. We can associate each point of the surface as a (x,y,z) coordinate.

Resolution (R) of the measurement establishes the number of points per lines, m , rows, n , and the dimensions of the measured area (A).

The step p of the measurement for x and y (p_x, p_y) are defined by :

$$p_x = \frac{l_x}{m} \quad (1) \quad \text{and} \quad p_y = \frac{l_y}{n} \quad (2)$$

With l_x and l_y the lengths of x and y for the total analysed surface

Often $p_x = p_y$ and $l_x = l_y$ (the number of data points remains the same along x and y)

Each AFM measurement plot H relates to a z value (in fact $z - z_0$) at one coordinate (x,y) and can be introduced inside a matrix format M :

$$M = \begin{pmatrix} z_{0,0} & z_{1,0} & \cdots & z_{i,0} \\ z_{0,1} & z_{1,1} & \cdots & z_{i,1} \\ \vdots & \vdots & \ddots & \vdots \\ z_{0,j} & z_{1,j} & \cdots & z_{i,j} \end{pmatrix} \quad (3)$$

The total specifically surface is mapped with the elementary surface defined by $z_{i,j}; z_{i+1,j}; z_{i,j+1}; z_{i+1,j+1}$ points as described in the figure 1 :

The area of $S_{e,p,i,j}$ is a constant and defined by the step of the measurement.

$$S_{e,p,i,j} = p_x \times p_y \quad (4)$$

Nevertheless, for many cases it's difficult to evaluate the elementary surface $S_{e,r}$. $S_{e,r}$ is defined as the decomposition of the elementary surface in two triangular elementary surfaces named T . There are two possibilities to decompose the $S_{e,r}$ to two triangular surfaces. Both cases are described in the figure 2 a) and b).

The triangular surface $T_{i,j}$ is delimited by the data points $(z_{i,j}, z_{i+1,j}, z_{i+1,j+1})$, $T_{i,j}^*$ by $(z_{i,j}, z_{i,j+1}, z_{i+1,j+1})$ and for the second possibility $G_{i,j}$ by $(z_{i,j}, z_{i+1,j}, z_{i,j+1})$ and $G_{i,j}^*$ by $(z_{i,j+1}, z_{i+1,j}, z_{i+1,j+1})$

The nomenclature employed for the elementary surface is represented in figure 3 In general cases, the triangles $T_{i,j}, T_{i,j}^*, G_{i,j}, G_{i,j}^*$ are not particular (equilateral, isosceles and rectangle). In fact, the determination of their surface is more difficult.

To determine the surface of the triangle S only by edges (good approximation except for very low angles triangles, if not use the Kahan relationship), we use the generic Héron of Alexandria relationship [9] :

$$S = \sqrt{d(d-a)(d-b)(d-c)} \quad (5)$$

where d is half perimeter of the triangle, a, b and c the length of side of the triangles. The application of the Héron formula in our case can be written as :

The edge of triangle are expressed by :

$$a_{i,j} = \sqrt{p^2 + (z_{i+1,j} - z_{i,j})^2} \quad (6) \quad \text{and} \quad b_{i,j} = \sqrt{p^2 + (z_{i,j+1} - z_{i,j})^2} \quad (7)$$

because of junction of T and T^* (similar for G and G^*), we can write $c_{T,i,j} = c_{T^*,i,j}$ (similar for $c_{G,i,j} = c_{G^*,i,j}$), however $c_{T,i,j}$ is only adapted for T and T^* triangles ($c_{G,i,j}$ for G and G^* triangles) :

$$c_{T,i,j} = c_{T^*,i,j} = \sqrt{2p^2 + (z_{i+1,j+1} - z_{i,j})^2} \quad (8)$$

The half perimeter is defined by:

$$d_{T,i,j} = \frac{a_{i,j} + b_{i+1,j} + c_{T,i,j}}{2} \quad (9) \quad \text{and} \quad d_{T,i,j}^* = \frac{a_{i,j+1} + b_{i,j} + c_{T,i,j}}{2} \quad (10)$$

The elementary surfaces S_T of triangles T and T^* defined by :

$$S_{T,i,j} = \sqrt{d_{T,i,j}(d_{T,i,j} - a_{i,j})(d_{T,i,j} - b_{i+1,j})(d_{T,i,j} - c_{T,i,j})} \quad (11)$$

and

$$S_{T,i,j}^* = \sqrt{d_{T,i,j}^*(d_{T,i,j}^* - a_{i,j+1})(d_{T,i,j}^* - b_{i,j})(d_{T,i,j}^* - c_{T,i,j})} \quad (12)$$

For triangles G and G^* , we can use $a_{i,j}, a_{i,j}^*, b_{i,j}, b_{i,j}^*$ but not c :

$$c_{G,i,j} = c_{G,i,j}^* = \sqrt{2p^2 + (z_{i+1,j} - z_{i,j+1})^2} \quad (13)$$

$$d_{G,i,j} = \frac{a_{i,j} + b_{i+1,j} + c_{G,i,j}}{2} \quad (14) \quad \text{and} \quad d_{G,i,j}^* = \frac{a_{i,j+1} + b_{i+1,j} + c_{G,i,j}}{2} \quad (15)$$

$$S_{G,i,j} = \sqrt{d_{G,i,j}(d_{G,i,j} - a_{i,j})(d_{G,i,j} - b_{i,j})(d_{G,i,j} - c_{G,i,j})} \quad (16)$$

$$S_{G,i,j}^* = \sqrt{d_{G,i,j}^*(d_{G,i,j}^* - a_{i,j+1})(d_{G,i,j}^* - b_{i+1,j})(d_{G,i,j}^* - c_{G,i,j})} \quad (17)$$

The total specifically surface represented by the average of (T, T^*) and (G, G^*) surfaces :

$$S_T = \frac{\sum_i^{m-1} \sum_j^{n-1} S_{T,i,j} + \sum_i^{m-1} \sum_j^{n-1} S_{T,i,j}^* + \sum_i^{m-1} \sum_j^{n-1} S_{G,i,j} + \sum_i^{m-1} \sum_j^{n-1} S_{G,i,j}^*}{2} \quad (18)$$

The ratio R of the specifically surface on measured area A is :

$$R_s = \frac{S_T}{A} \geq 1 \quad (19)$$

2.2. Program source

From one software to another one, files exist that are not always structured in the same way. For this reason it is necessary to extract the topological data that are always represented in a column (figure 4).

The first phase of data treatment consists of transforming the column of data (vectorial matrix) into a matrix $m \times n$. This matrix is directly the representation of

the topological surface in amplitude. The interval between two consecutive matrix components corresponds to the AFM measurement increment.

The second phase of the program consists in determination of the vectors $a_{i,j}$, $b_{i,j}$ and $c_{i,j}$ in order to calculate the elementary surface corresponding to a package (four matrix points correspond to a package) and to fully define it.

Thus, a surface value is extracted, but a point of reference has not been defined. For a better comparison between the calculated surfaces, the surface will be divided by the entire surface of projection.

2.3. Basic analyses of easy surface

To verify the efficiency of our program, we must analyse some simple surfaces (named reference surfaces) such as square flat plane surface, a xy slope plane, pyramid surface, half sphere and random surfaces. Except for the half sphere and pyramids, all surfaces are described with 10^4 data points.

2.3.1. The flat square plane surface

The easy surface is a square flat plane. If L is a side of square of the flat plane, the surface is L^2 , then the theoretical surface ratio R_{Th} is defined by :

$$R_{Th} = \frac{L^2}{L^2} = 1$$

Such calculating R value is equal to one for any resolutions.

2.3.2. The xy plane slope

The slope of a xy plane is defined by the equation $z = x + y$. Mathematically :

$$R_{Th} = 1.2246$$

The result obtained by our program is :

$$R_{prgm} = 1.22068$$

There is a good agreement between the mathematical calculation and the program (the relative error reminds below 0.3%).

2.3.3. The Pyramidal surface

- One pyramid only

One pyramid, defined with three different resolutions has been used in the program to determine the evolution of the error with the resolution. The height of the pyramid is 8 units.

$$R_{Th} = 2.2361$$

The program can't exactly evaluate the specifically surface because of the average of the surface with both configurations which include the little steps along the edge of the pyramid. The value of the specifically surface depends on the resolution. The relative error is reported as a function of the resolution in figure 5. We noticed that the R_{prgm} values gradually converge to R_{Th} . Only 0.5% relative error is obtained with 1000 data points and justified the good results of the program.

- Multiple pyramids covering the entire surface

2500 pyramids of 1 unit height, is the maximum allowed for complete coverage of the surface, the theoretical ratio of the specifically surface over this area is $1.4142 (\sqrt{2})$. R_{prgm} is equal to 1.39012.

For an extreme case, with pyramids at a height of 100 units, the theoretical ratio of the surface is 100, the program gives 85.60. This difference becomes important but it's not a specifically case (extreme case).

2.3.4. The full space half sphere

The theoretical value of the surface ratio of the full half sphere is defined by :

$$R_{Th} = \frac{\pi \times r^2 + L^2}{L^2} \quad (20)$$

In our case L (the edge of the studied domain) and r the radius of the half sphere is $L = 2r$.

$$R_{Th} = \frac{\pi}{4} + 1 \approx 1.7853$$

We investigate the evolution of the R values with the half sphere resolution for six cases as shown in figure 6. The evolution of the relative error as a function of the total number of data points is described by the graphic representation in figure 7.

It shows that the resolution is a fundamental parameter, the shape must be described by more than 1000 data points to have a negligible relative error. The relative error is more important than in the pyramid case and explained by the non linear interpolation between two points in the case of the spherical shape.

2.3.5. The random surfaces

We defined a surface by 100×100 data points and calculated the surface ratio R_{prgm} for two cases. For the first one with a random $[0,1]$ amplitude, the value of the

surface ratio R calculated by the program is 1.148 for the second one with a random [0,100] amplitude, the value of the surface ratio R_{prgm} is 52.24. The variation of the R value for both cases is very low.

3. Experimental applications

3.1. Particular experimental surface case

A $\text{YBa}_2\text{Cu}_3\text{O}_7$ thin film made by pulsed laser deposition technique has been characterized by AFM (PicoSPM). The film shows a particular surface (cf fig 8) with simple shapes (prismatic batons) [5] with which the specifically surface can be estimated with an easy mathematic calculation. The rms roughness of the film is 3.2 nm, the maximum peak valley is 19.6nm. We estimate 85 batons at the surface of the film. The average size of batons are : width ($l = 42$ nm), high ($h = 8.75$ nm) and length ($L = 102.6$ nm), the batons have a prismatic shape. The angle of the slope of the base surface is about 3.27° . The surface baseline ratio calculated with the slope angle is : $R_{\text{baseline}} = 1.002$.

The surface ratio contribution of batons is :

$$R_{\text{batons}} = \frac{n \times s_{\text{batons}} - n \times ps_{\text{batons}}}{1000^2} \quad (21)$$

where n is the number of batons, s_{batons} the batons area and ps_{batons} the projected batons area on the base surface.

$$R_{\text{batons}} = 0.0303$$

Finally the estimated value of the surface ratio R is

$$R = R_{\text{baseline}} + R_{\text{batons}} = 1.032$$

R_{prgm} is equal to 1.028. The difference between the value calculated by the program and the theoretical calculation is rather small (the relative error is 0.4%) and justify the validity of the program. The authors obtained $R = 1.043$ with the Gwyddion open source program [3], it show a pretty good agreement result between both programs.

3.2. Complex experimental surface case

A 450 nm ZnF_2 thin film grown by pulsed laser deposition technique has been analysed by AFM (see the figure 9). The roughness of the film is very high (The rms roughness is 35.65 nm [10], the maximum peak valley is 216 nm). The surface ratio of the film calculated by our program is $R_{\text{prgm}} = 2.423 \pm 1.12 \times 10^{-3}$. This value is more important than the value determined for the YBCO thin film.

This result is in agreement with the roughness and morphology difference between both films.

3.3. Discussion about the surface measurement limitation

The amplitude limitation of the AFM measurement, the resolution and the shadows effects generate errors of the specifically surface values given by the program. The results from the program give always underestimated values (more or less in agreement with the morphology profile and the resolution) due to the absence of the data point definition located between (i,j) and $(i+1,j+1)$. The limitation of the apparatus resolution is very important because defects size below the step sizes aren't taken into account and do not influence the result. For this reason, it's preferable to work with the maximum resolution [7]. Everything under the measured surface such as the close porosity is not considered in the program. There is no influence of these elements on the R_{prgm} .

4. Conclusion

In this paper, we developed a new program which permits to determine the specifically surface of thin film with the AFM data. This program improves the morphology and topography characterization of samples (addition of rms roughness, FFT and maximum amplitude). This technique must be used with high resolution data points. A resolution of the surface shapes defined with 1000 data points is enough for a specifically surface calculation with high accuracy. Nevertheless, this technique can't directly determine the almost closed nanopores under a surface. The specifically surface determined by the program always remains underestimated to that of the true value.

A potential application is the determination of the internal porosity of the thin films by the difference between the specifically surface calculated by our method and the volume measured by picnometry. Our program is a key tool for many applications dealing with surfaces such as gas sensors.

Acknowledgements

The authors want to thank A. Rougier and D. Larcher for their helps and C. McLoughlin for the writing corrections and the EU program INTERREG IVA 2-Seas (CleanTech project).

References

- [1] F. Sánchez, M.V. Garcia-Cuenca, C. Ferrater, M. Valera, G. Herranz, B. Martinez, J. Fontcuberta, *Applied Physics Letters* **83**, 902-904 (2003)

- [2] G. Binning, C. F. Quate, C. Gerber. Phys. Rev. Lett. **56** (9), (1986) 930
- [3] Gwyddion open source software (<http://gwyddion.net/>)
- [4] N. Yao, Z.L. Wang. Handbook of Microscopy for Nanotechnology (2005)
- [5] P. Bernstein, J. Mosqueira, J. Siejka, F. Vidal, Y. Thimont, C. McLoughlin G.Ferro, Journal of Applied Physics **107**, 123901 (2010)
- [6] S. Bau, O. Witschger, F. Gensdarmes, O. Rastoix, D. Thomas, Powder Technology. 200 (2010) 190-201
- [7] U. D. Schwarz, H. Hölscher and R. Wiesendanger, Phys Rev **B62**, 13089 (2000)
- [8] U. Lüders, F. Sanchez, J. Fontcuberta, Phys. Rev. **B70**, 045403 1-6 (2004)
- [9] W. Kahan, Math. Dept., and E. E. and Computer Sci. Dept. University of California, Berkeley CA 94720-1776
- [10] Y. Thimont, J. Clatot, M. Nistor and A. Rougier, From ZnO to ZnF₂ thin films using Pulsed Laser Deposition, in preparation.

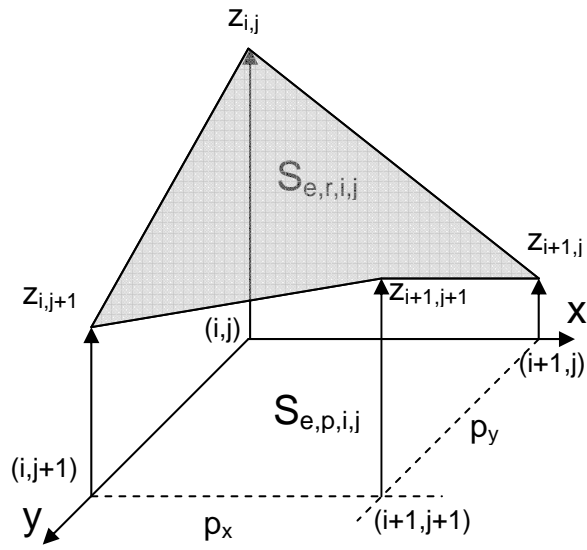


FIG. 1. The elementary surface ($S_{e,r}$) and the projected surface elementary ($S_{e,p}$).

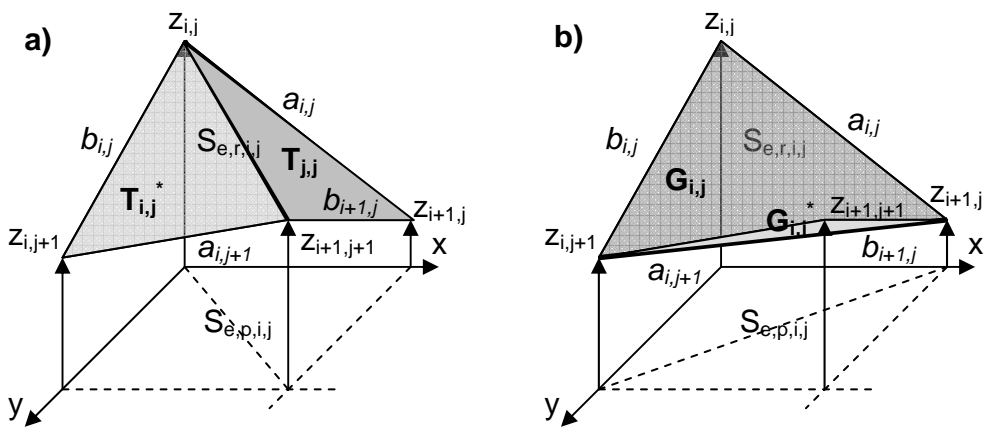


FIG. 2. Decomposition of the $S_{e,r}$ in two triangular elementary surfaces with the first possibility a) and the second b).

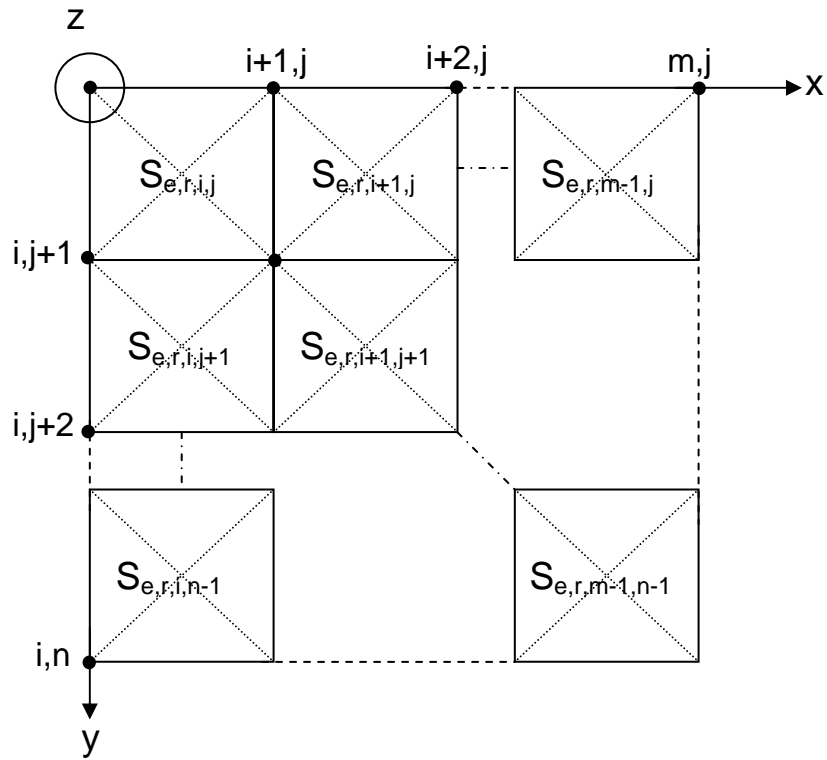


FIG. 3. Nomenclature of the elementary surface in (x,y) plane projection

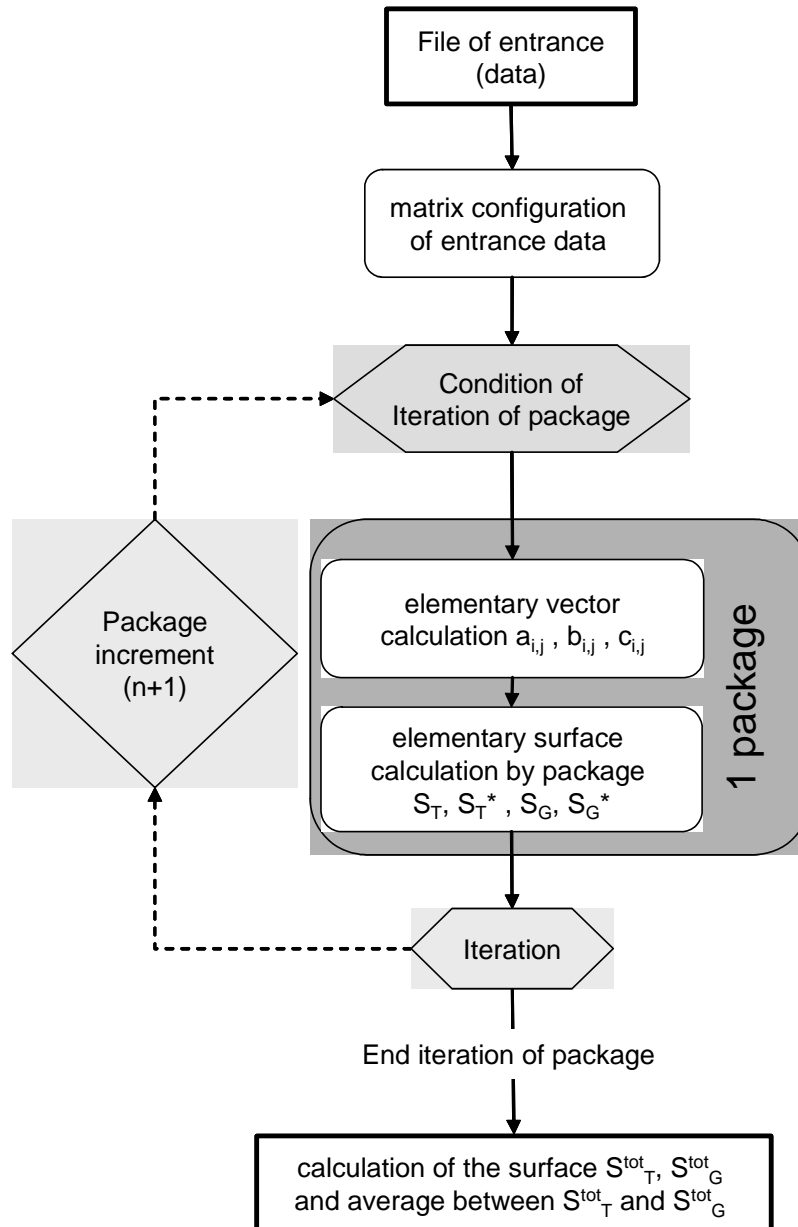


FIG. 4. Slowchart of the structure of the file programs presenting the important stages of the numeric calculation. A package represents an elementary matrix (2x2) which terms are $(z_{i,j}, z_{i,j+1}; z_{i+1,j}, z_{i+1,j+1})$. Two types elementary surfaces are calculated by package (S_T, S_T^* and S_G, S_G^*)

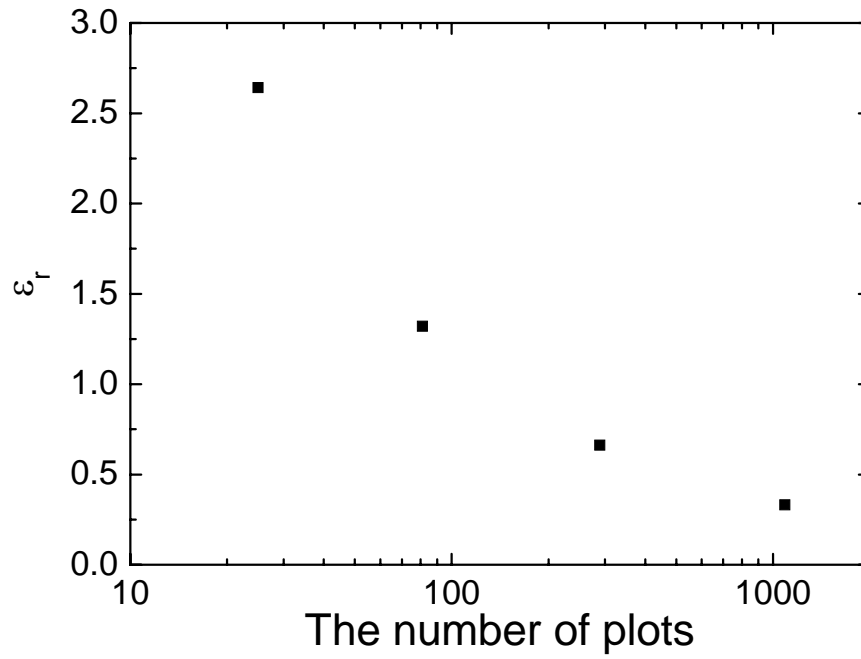


FIG. 5. The evolution of the relative error with the total number of plots for the pyramid shape.

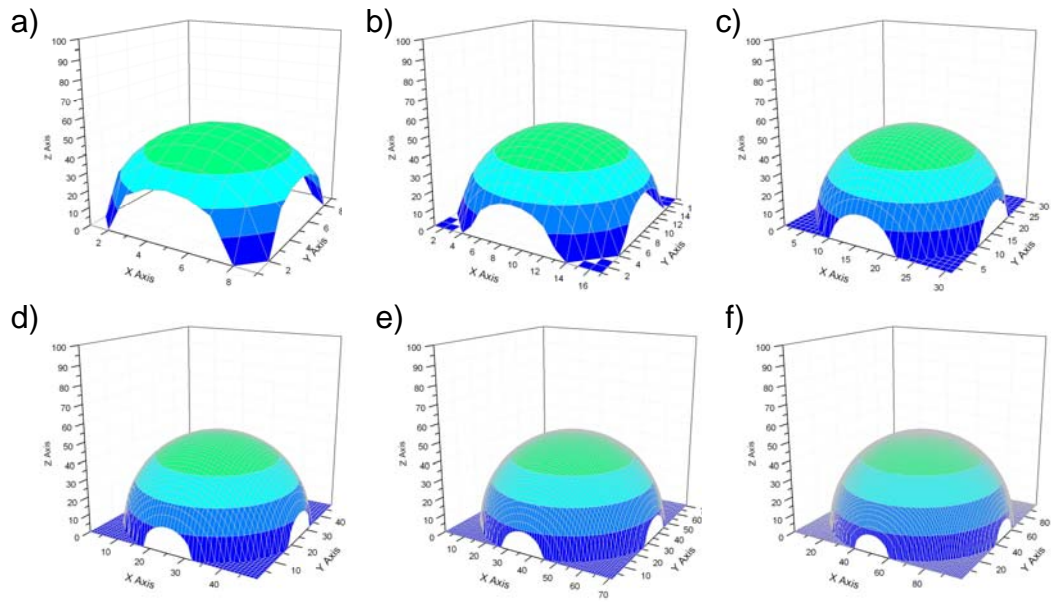


FIG. 6. Multiple half spheres with different resolutions : a) 81 data points, b) 289 data points, c) 961 data points, d) 2401 data points, e) 5041 data points and f) 9801 data points).

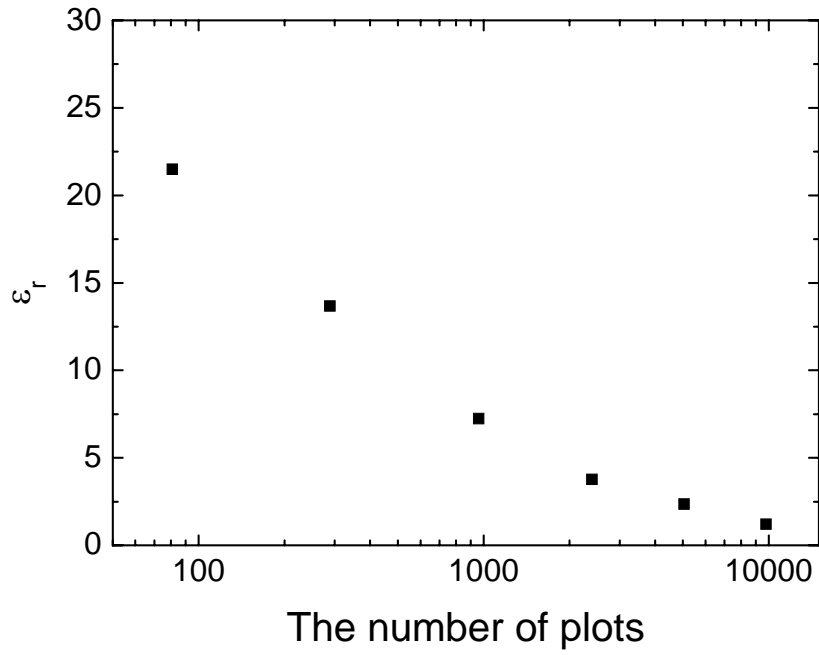


FIG. 7. The evolution of the relative error with the total number of data points for the half sphere.

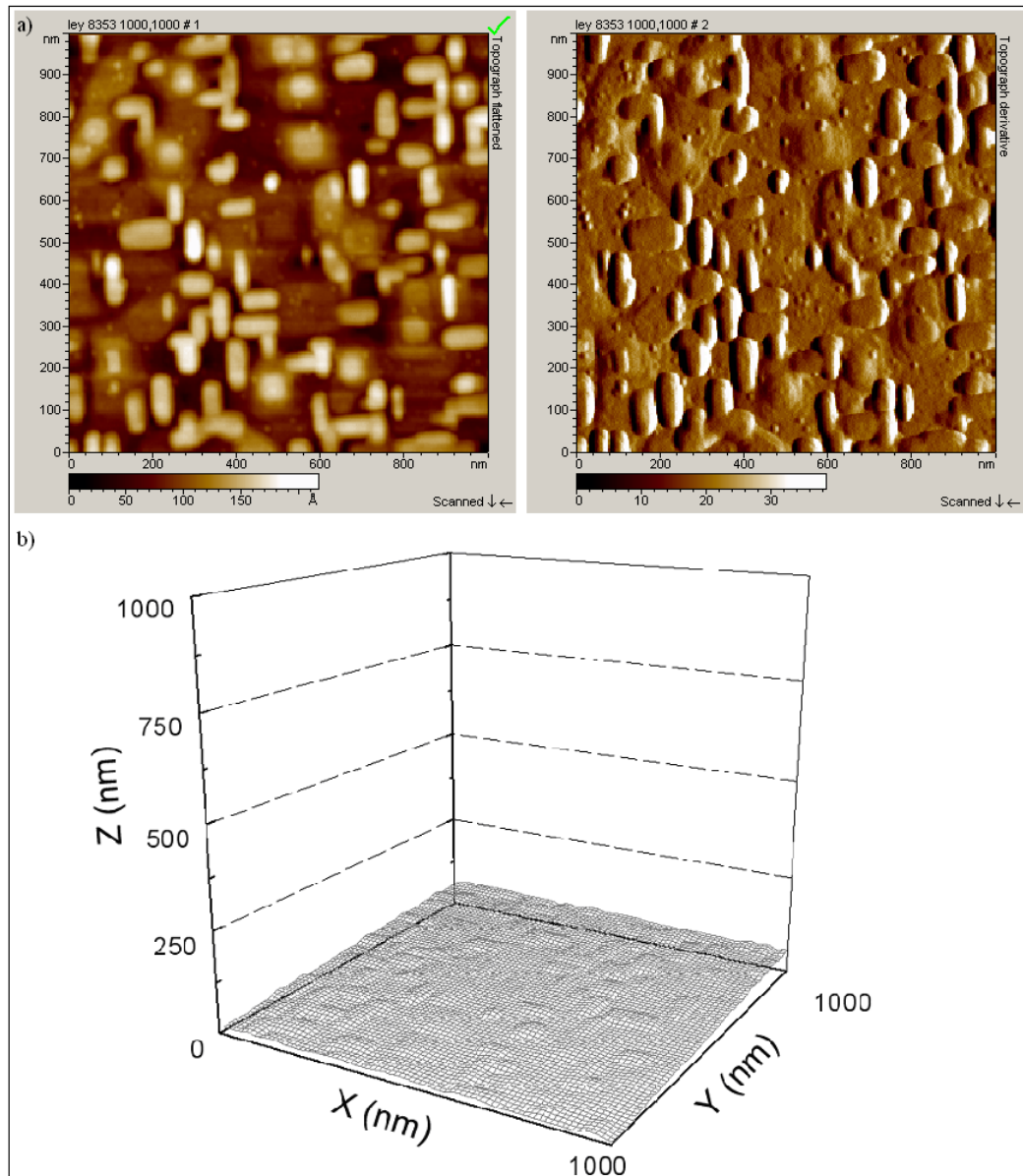


FIG. 8. Batons on the YBCO thin film surface a) The direct row image from AFM measurement at left and the derivative image at right and b) reported in isoscale (x,y,z) representation (the number of dots have been limited to simplify the picture).

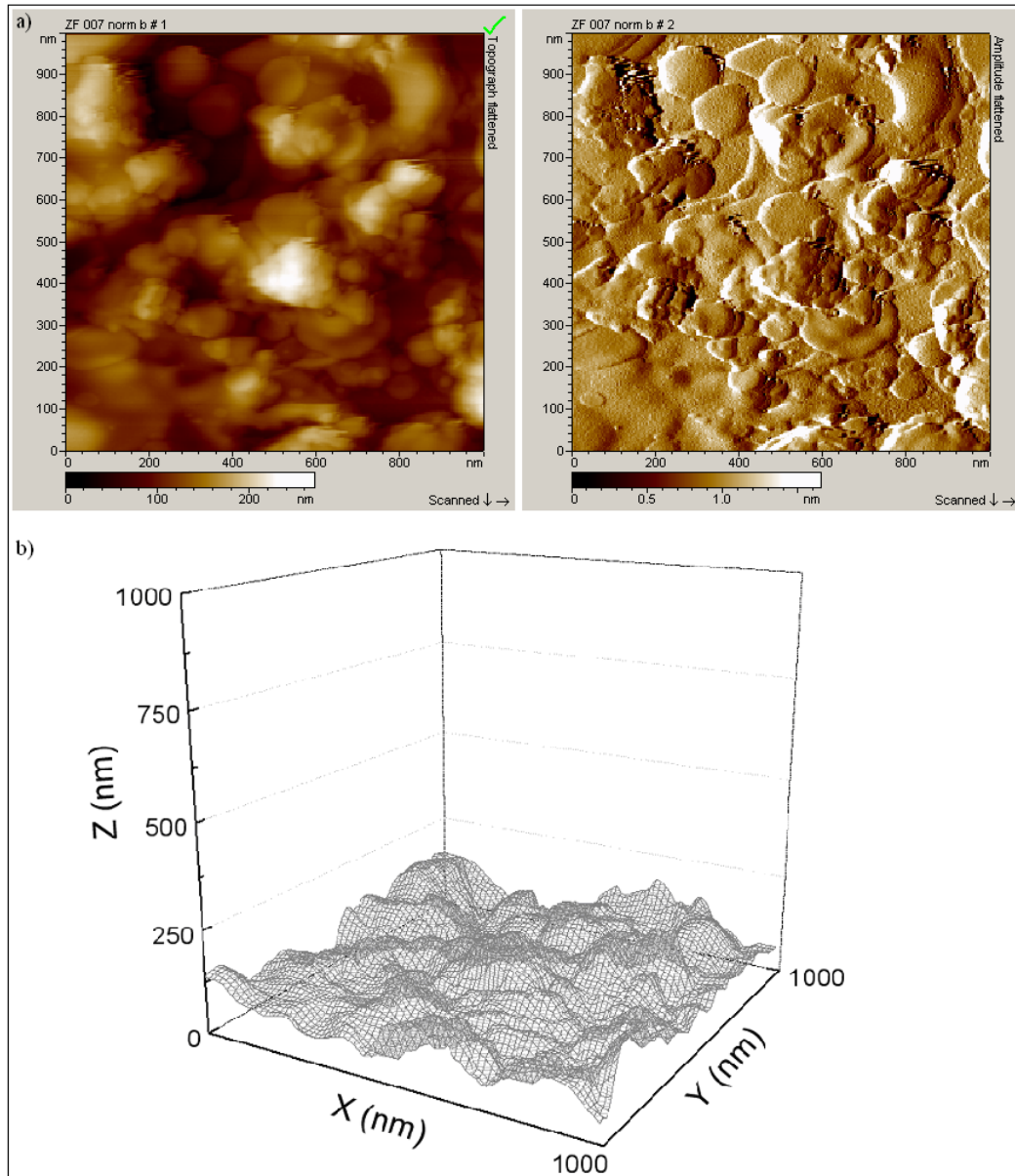


FIG. 9. The ZnF₂ thin film surface a) The direct row image from AFM measurement at left and the derivative image at right and b) reported in isoscale (x,y,z) representation (the number of dots have been limited to simplify the picture)

Received: November, 2012